

## Flow and torsional oscillator measurements on liquid helium in restricted geometries under pressure

Cao Lie-zhao,\* D. F. Brewer, and C. Girit†

*Physics Laboratory, University of Sussex, Brighton BN1 9QH, United Kingdom*

E. N. Smith and J. D. Reppy

*Laboratory of Atomic and Solid State Physics and Materials Science Center,  
Cornell University, Ithaca, New York 14853-2501*

(Received 26 April 1985)

When a solid surface is in contact with liquid helium, the strong van der Waals forces between helium and the solid substrate result in a layer of high-density helium localized on the substrate. It was expected that, upon raising the pressure, further solid layers would grow out from the wall. Many experiments have now shown that this usually does not occur, and even at solidification pressures  $^4\text{He}$  liquid, rather than solid, wets a disordered surface. This implies that, in the neighborhood of some solid surfaces, liquid helium can exist at pressures above bulk solidification pressure. We have devised two experiments, using dc superflow and torsional oscillator methods, to investigate this effect in the confined geometries of Vycor and fine powders. In the dc flow method, which relies on the detailed form of the He I–He II–solid-phase diagram, the outer ends of a rod of Vycor or other material are left in the superfluid region while the center is in the bulk solid region. We confirm that superflow takes place through this system, and observe new phase diagrams showing where superflow can occur in several materials of different pore size. The torsional oscillator consists of a Vycor cylinder encapsulated in a beryllium copper container with a Be-Cu torsion tube through which helium can be admitted. In the bulk fluid region we confirm that the superfluid transition in Vycor occurs at temperatures  $T_0$  which are parallel to, but lower than, the bulk  $\lambda$  line. At higher pressures, in the bulk solid region,  $T_0$  is found to propagate up into the bulk solid region as high as 25 bars above the bulk solidification pressure. The superfluid mass in Vycor cannot be calculated unambiguously, but it can be inferred that at absolute zero it decreases slowly between zero pressure and 30 bars, and thereafter more rapidly, becoming zero at about 50 bars. We suggest that the failure of solid to nucleate at the surface is due to its amorphous nature which discourages the formation of crystallites, and that a high-density disordered phase nucleates within the fluid in the pores according to a well-known nucleation theory which gives the correct order of magnitude for the overpressure required. This implies the existence of a high-density localized state of helium which is disordered even at 0 K. An observation which we have not as yet been able to explain is a falloff in period of the torsional oscillator at the solidification curve as the temperature is reduced at constant pressure, starting in the normal fluid phase. This phenomenon is observed with  $^3\text{He}$  as well as with  $^4\text{He}$ .

### I. INTRODUCTION

It is well known that the relatively large van der Waals attraction between helium and a solid surface, together with the high compressibility of fluid helium, result in an adsorbed film at low temperatures whose density close to the wall is considerably larger than that of bulk liquid.<sup>1</sup> Theoretical treatments of this effect have been given,<sup>2,3</sup> and several experiments confirm it.<sup>1,3,4</sup>

A natural outcome of this observation is to expect that when the pressure in a vessel containing liquid helium is increased, solid helium will grow out from the wall even at pressures below the bulk solidification pressure,  $p_m$ . Mitchell *et al.*<sup>5</sup> attempted to exploit this idea for a new refrigeration technique by immersing a highly porous material (Vycor porous glass,<sup>6</sup> also used in the present work)

in liquid  $^3\text{He}$  and carrying out a Pomeranchuk cooling experiment. The aim was to achieve cooling through solidification of  $^3\text{He}$  within the Vycor at pressures  $p < p_m$  which would then cool the bulk liquid outside the pores, also at  $p < p_m$ , below the superfluid transition temperature ( $< 2.65$  mK). The experiment, which started at an initial temperature of about 40 mK, was partly successful, but solidification was not observed at the low pressures expected.

Other experiments also failed to detect the growth of solid layers on substrates at pressures below  $p_m$ . Following the unexpected result of the modified Pomeranchuk cooling experiment, Brewer *et al.*<sup>7</sup> used a different approach to examine the possible growth of  $^4\text{He}$  solid on the same substrate (Vycor) at higher temperatures ( $\sim 1.5$  K). Their method was to measure as a function of pressure

the frequency  $\omega$  of superfluid oscillations between two reservoirs connected by a Vycor superleak. The frequency is given by an expression  $\omega^2 \propto (\rho_s/\rho)_{\text{ch}}(a/l)$ , where  $(\rho_s/\rho)_{\text{ch}}$  is the superfluid fraction in the channel, and  $a/l$  is the effective ratio of area to length of the porous Vycor. Growth of solid from the wall would be expected to reduce  $a/l$  in a way that could be calculated from the simple theory.<sup>3</sup> Although this experiment was complicated by the fact that  $(\rho_s/\rho)_{\text{ch}}$  is also expected to be a function of  $a$ , it could nevertheless be inferred that the observations were not consistent with the growth of solid at low pressure as given by theory.

The same conclusion was drawn from experiments by Berthold *et al.*<sup>8</sup> and Bishop *et al.*,<sup>9</sup> who used one of the techniques which we describe in this paper—the modified Andronikashvili oscillator developed extensively at Cornell University—to measure the superfluid mass in Vycor of <sup>4</sup>He films and liquid under pressure. Early observations<sup>10</sup> in Pomeranchuk cells had, in addition, suggested the possibility of liquid supercooling, i.e., the existence of liquid <sup>3</sup>He at pressures above  $p_m$ . Surface tension experiments by Balibar, Edwards, and Laroche<sup>11</sup> showed that, for a particular substrate (copper), the <sup>4</sup>He liquid-substrate free energy (at around 1 K) was lower than the solid-substrate free energy, so that the liquid wetted the substrate in preference to the solid, and the solid <sup>4</sup>He meniscus in a copper tube was depressed. In a very different type of experiment on viscosity and positive ion mobility near the solidification pressure of liquid <sup>4</sup>He, Scaramuzzi *et al.*<sup>12</sup> interpreted their observations as indicating that the  $\lambda$  line extends into a supercooled liquid region above the solidification pressure.

These experiments show that, although the first adsorbed layer is tightly bound at solid density, certain surfaces inhibit the formation of further solid layers, and that this effect may persist significantly above the bulk solidification pressure. In order to test this speculation, we devised experiments to observe superflow in liquid <sup>4</sup>He at pressures above  $p_m$ , and to measure the superfluid mass by the torsional oscillator technique. Preliminary measurements<sup>13,14</sup> confirmed the existence of fluid at pressures of several bars above  $p_m$ , and demonstrated an interesting reduction in the superfluid fraction at higher pressures. The first experiments studied specifically the behavior of helium confined in Vycor, while subsequent work also incorporated packed powders<sup>6</sup> in which the pore size could be varied. In the present paper we give a detailed account of this work.

Following the initial experiments many more observations, in our own laboratories and elsewhere, have confirmed and extended the work. Specific-heat measurements were made simultaneously by Thomson *et al.*<sup>15</sup> and have since been considerably extended and include <sup>3</sup>He.<sup>16</sup> Isochore measurements, demonstrating directly the existence of the “internal melting curve” have been made by Smith *et al.*,<sup>17</sup> Adams *et al.*,<sup>18</sup> and Thomson *et al.*<sup>19</sup> Beamish *et al.*<sup>20</sup> have used ultrasonic techniques as a probe. Further investigations of the effect in <sup>3</sup>He have been made by Shimoda *et al.*<sup>21</sup> using NMR and specific-heat methods, while Adams *et al.*<sup>18</sup> have extended their isochore measurements to this new isotope. Lea and Fo-

zumi,<sup>22</sup> although not making measurements above  $p_m$ , have also added evidence, in ultrasonic measurements, that solid growth at low pressures does not occur on a substrate of gold-plated quartz.

Some experiments show that high-density helium, not necessarily solid, does form on some surfaces, possibly depending on whether the crystal structure of the surface and the solid helium phase are commensurate. We return to this question in the later discussion.

## II. FLOW EXPERIMENTS

A broad range of flow experiments has now been carried out in the extended liquefaction region for helium in porous media. All are similar in principle of operation to the first of these which was performed using a 3-mm-diam. rod of porous Vycor glass as the helium confinement medium. The apparatus for this experiment is schematized in Fig. 1. The Vycor rod is epoxied into a thin-walled stainless-steel tube, with the central portion thermally anchored to a <sup>3</sup>He refrigerator. Capillary fill lines admit <sup>4</sup>He to the end of the Vycor rod, and are thermally anchored to one another and to a pumped <sup>4</sup>He refrigerator. As the small pore size in the Vycor restricts two-fluid counterflow, it is possible to maintain large temperature gradients along the flow channel even below the superfluid transition. The “inlet” capillary is connected to a room-temperature supply of pure <sup>4</sup>He gas which is passed through a pressure regulator, LN<sub>2</sub> trap, pressure gauge, and valve before being admitted to the cryostat. The “outlet” capillary is connected to a capacitive strain gauge mounted at 4.2 K, and at room temperature to a valve and rotary pump. In operation, the apparatus was cooled down to below 1.5 K and helium was condensed into the system to a pressure of a few bars. After thermal equilibration was achieved, one could examine whether there was superfluid present in the Vycor section by making a small pressure modification in the inlet side and looking for a pressure response on the outlet side. With superfluid present in the Vycor flow channel, there was rapid pressure equalization between the two sides of the

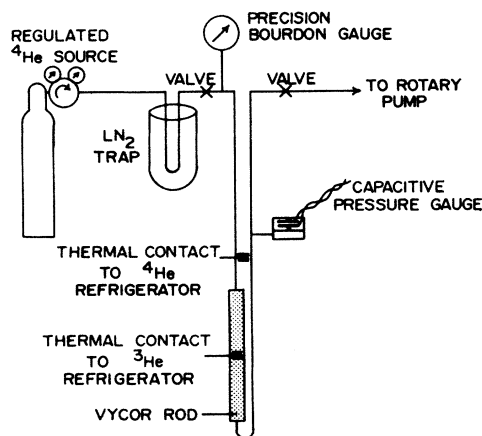


FIG. 1. Schematic diagram of flow apparatus used in initial experiments.

Vycor. At more elevated temperatures, the normal fluid viscosity was sufficient to block any pressure response on the outlet side, within the pressure sensitivity and time limitation of the experiment. Thus, by varying the temperature of the central portion (or the ends) of the Vycor it was possible to map out the superfluid transition temperature as a function of pressure for helium in Vycor glass, as shown later in Fig. 13. The bulk solidification curve<sup>23</sup> and  $\lambda$  line<sup>24</sup> are well established in the literature, as is the depression of the  $\lambda$  line by the presence of a reduced geometry,<sup>1</sup> although the exact amount is strongly dependent on pore size. The present data is in good agreement with previous work at pressures below the usual melting pressure.

The new feature demonstrated in this experiment was the extension in Vycor of the liquid portion of the phase diagram to pressures above the bulk melting curve. The experimental technique utilized is most easily understood with reference to Fig. 2. The ends of the Vycor segment are maintained at a temperature and pressure indicated by the point *A* on this figure, which leaves the helium in the fill capillaries liquid and superfluid, and also leaves the helium in the Vycor at the inlet ends in a superfluid state. The center of the Vycor rod is then cooled to temperatures as low as  $\sim 0.5$  K with the  $^3\text{He}$  refrigerator. At various temperatures, tests of superfluidity were made by adjusting the pressure slightly on the inlet and looking for response at the outlet pressure gauge. No indication of solidification was observed, even at pressures which were more than a bar greater than the bulk melting curve at the low-temperature end. It was possible to measure the bulk

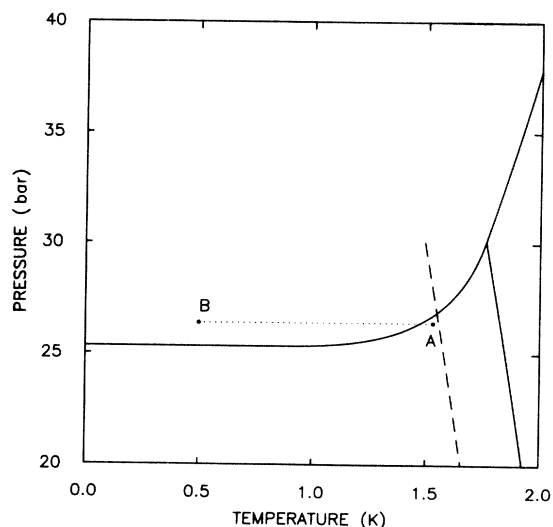


FIG. 2. Phase diagram for  $^4\text{He}$ . Ends of the flow channel are kept at point *A*, where the temperature and pressure are such that the fill lines contain superfluid liquid helium, and the helium at the ends of the Vycor is also superfluid. The temperature of the center of the flow channel, point *B*, may be varied along the dotted line. Except for rather small fountain pressure effects, the pressure is constant along the flow channel.

melting pressure directly by cooling the ends of the Vycor rod until freezing of the bulk liquid in the fill lines occurred, eliminating pressure contact between the two sides. The satisfactory agreement between these results and published values<sup>23</sup> for the melting curve provide a check on both the pressure calibration and the thermometry.

A limitation to the scope of these measurements was the amount by which the helium can be overpressurized above bulk melting, while still retaining superfluidity in the inlet sections of the apparatus. A natural extension of the experiment was, therefore, to pack the inlet sections with powder of larger pore size than Vycor, and thus to reduce the depression of the superfluid transition. At the same time the apparatus was modified to provide greater sensitivity and added convenience of measurement. The modified apparatus is shown schematically in Fig. 3. The principal new feature is a small additional volume on the inlet side of the superleak which was weakly coupled to 4.2 K, and whose temperature could be easily modulated by injection of a few mW into a heater. Using the temperature variation of the molar volume of the helium in this appendage then gave a convenient method of producing small pressure undulations of a few mbar about a fixed average pressure. As the temperature of the central portion was raised, for example, one could see the pressure response of the strain gauge on the far side and cease to see pressure contact over the range of a few mK as the superfluid transition was crossed. A typical trace is shown in Fig. 4. The reduction in amplitude of transmitted oscillation is presumably related to either reduction of superfluid density or critical velocity in the region near the transition.

Results of both superfluid transition measurements and melting and freezing transitions are indicated in Fig. 5. It is seen that for all of the materials used,<sup>6</sup> including amorphous carbon, rouge, and alumina powders, there was an inhibition of complete blockage of the pores by solid formation. It may also be noted that the superfluid transi-

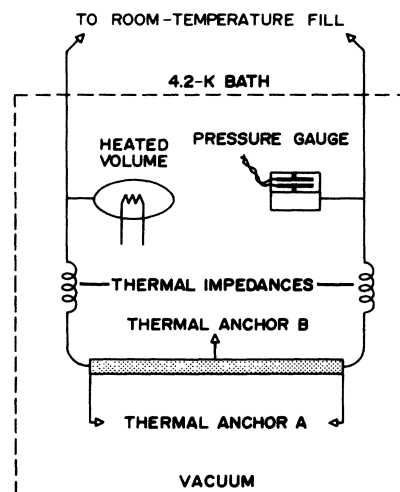


FIG. 3. Modified apparatus, with separate volume and heater used to create small pressure fluctuations at low temperatures.

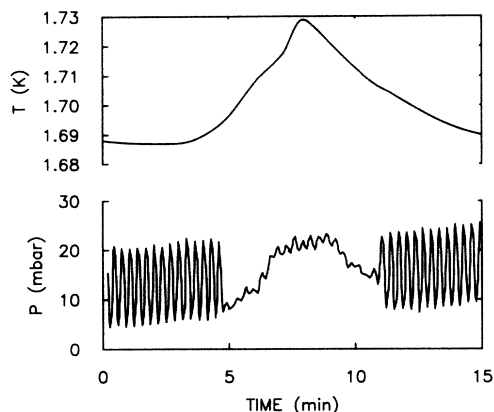


FIG. 4. Curves showing the time evolution of pressure response of the system as the temperature is ramped up and down through the superfluid transition region. The superleak is packed with 500-Å alumina, and the pressure scale shows relative pressure changes at a mean pressure of about 29 bars.

tion curve for the smallest pore sizes (in Vycor glass—a different sample from that described in Fig. 12, and with presumably slightly larger pores, and in a nominal 90-Å carbon powder, Carbolac 1) is extended to much higher

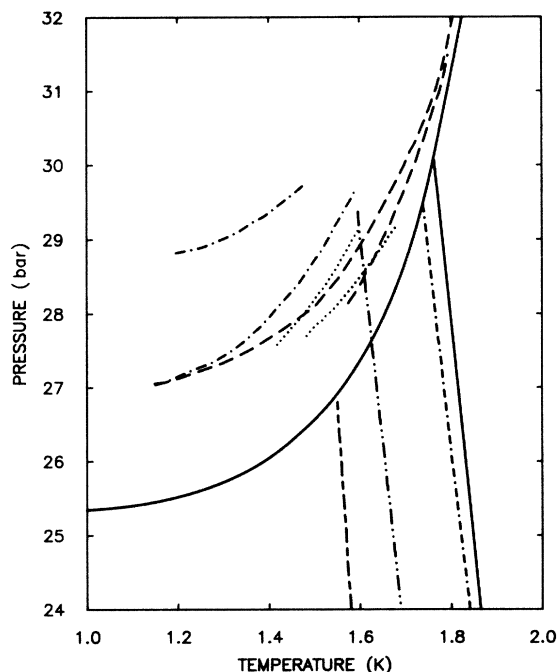


FIG. 5. Melting and freezing transitions are shown for the larger pore sizes investigated. Superfluid transitions are shown for a number of samples. Dashed-dotted line, 500-Å alumina, melting and freezing; long-dashed line, 3000-Å alumina, melting and freezing; dotted line 500-Å Nuclepore, melting and freezing; long-dashed—short-dashed line, Vycor, superfluid transition; dashed—double-dotted line, 90-Å carbon black, superfluid transition; double-dashed—dotted, 200-Å rouge, superfluid transition; solid lines, bulk melting curve and superfluid transition.

pressures than before. This was achieved, as explained above, with the use of a composite structure, filling the superleak at the middle with a small-pored structure, and at the ends with a larger-pored structure. Since our early measurements showed that 200-Å rouge produces very little suppression of superfluidity, while still preventing formation of solid below 30-bars pressure, this material was used at the inlet sections of the superleak.

The melting and freezing transitions were observed to be hysteretic for the 500- and 2000-Å alumina powders, with a greater deviation from bulk behavior for the smaller pore size. The magnitude of the superpressurization required (several bars in the 500-Å powder case) will be seen in the theoretical discussion of results to be in qualitative agreement with an approximate “model” which we have proposed for the system behavior.

The variation of pore size is clearly much larger for the systems of packed powders than in the Vycor glass. In an attempt to study a system with a narrow range of channel sizes an additional experiment was performed with a sandwich of 500-Å Nuclepore filter material enclosed between conventional packed-powder superleaks, Fig. 6. The pore size in the powder was much less than 500 Å so the melting and freezing of the helium was confined to the pores of the Nuclepore filter. Other studies<sup>25</sup> have shown Nuclepore to have a very narrow distribution of pore sizes. The resulting freezing-melting curves were intermediate between those for the 500- and 2000-Å packed powders, and again a substantial hysteresis between freezing and melting was evident.

A further effort was made to examine the effect in a packed powder of fluorocarbon powder DLX6000 (Ref. 6) with typical particle size of 2000 Å. This experiment turned out to be unsuccessful with our normal apparatus because of thermal contact problems. The fluorocarbon powder has a much greater thermal expansion coefficient than the walls of the superleak (unlike the other materials used), so that cracks apparently opened in the structure upon cooling from room temperature. This permitted superfluid counterflow, and made it impossible to establish a temperature gradient along the length of the flow tube.

All of the materials investigated in this sequence of measurements have been insulators. Sinters of very fine metallic powders of the sort often used in heat exchangers

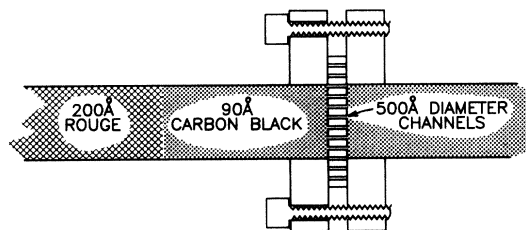


FIG. 6. Schematic view of apparatus for examining solid suppression in a piece of Nuclepore filter sandwiched between packed powder, not to scale. The thin sheet of filter paper serves both as a set of flow channels, and as a gasket sealing between the superleak and the vacuum can.

would be another material of interest for investigation. However, work elsewhere<sup>18</sup> using isochore measurements has shown that the behavior in these systems is fundamentally similar. A further category of investigation which might be of interest is to use small particles of graphitized rather than amorphous carbon, as it has been shown in various studies<sup>26</sup> that a quasiepitaxial growth of hcp helium takes place on graphite surfaces, which might well eliminate the solidification suppression. On the other hand, misalignment between microcrystallites nucleated on different sides of a pore might still prevent normal growth of a helium crystal in these small pores.<sup>27</sup> Unfortunately, as extreme cleanliness of the surfaces is needed to nucleate the solid growth, only the absence of solid suppression would be a definitive result.

### III. ISOCHORE MEASUREMENTS

We have also performed a series of pressure measurements of a constant volume sample as a function of temperature.<sup>17</sup> Isochore measurements of this type have also been performed elsewhere<sup>18,19</sup> with a somewhat different experimental arrangement. Our experiments were carried out in the sample chamber shown in Fig. 7. The body of the strain gauge was made from Berylco 25 alloy, with one wall forming the diaphragm of a capacitive pressure transducer. The internal volume of this part was about  $0.6 \text{ cm}^3$ , and filled to a packing fraction of 25% with Carbolac 1 powder of a nominal 90-Å pore size. Superleaks comprised of 2.5-mm stainless-steel tubes about 5 cm long packed with the same powder connected the pressure gauge to external fill lines, with various heat sinks along the length to permit variation of the temperature profile. Once the small (0.1 mm) diameter fill lines containing bulk liquid became blocked with solid, the helium in the carbon black formed essentially a constant volume system. Pressure was then measured as a function of temperature. The anticipated result had been that the pressure would remain essentially constant upon cooling through the bulk melting curve, then exhibit an abrupt drop to a new plateau as a freezing transition was reached. It was then anticipated that we would see substantial hysteresis on rewarming to higher temperatures. Qualitatively, this is what we saw as shown in Fig. 8. However, the pressure change associated with the presumed freezing transition was spread over a greater range in temperature than we had anticipated, perhaps because of the substantial range

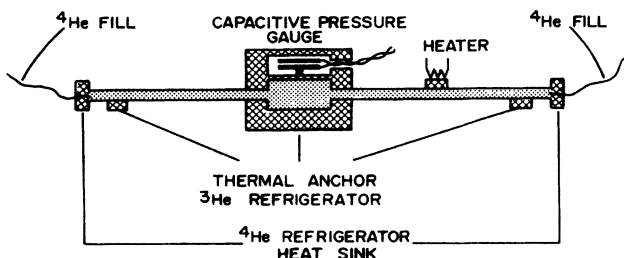


FIG. 7. Apparatus used for measurement of  $p(T)$  at constant volume for  $^4\text{He}$  confined in 90-Å carbon black powder packed to approximately 25% packing fraction.

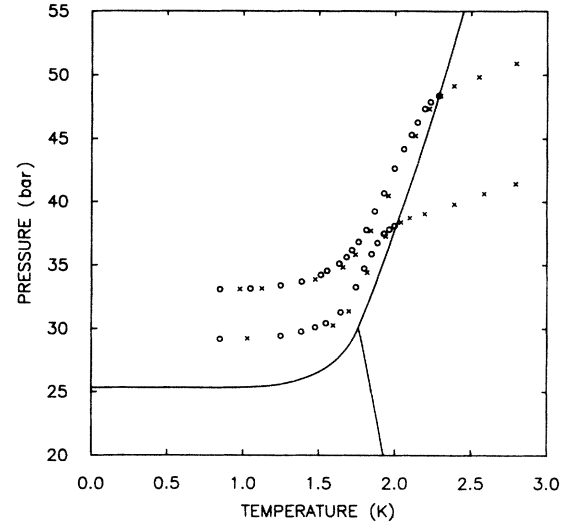


FIG. 8. Results of isochore measurements on  $^4\text{He}$  in carbon black, with two initial molar volumes for the  $^4\text{He}$ . Open circles indicate cooling; crosses indicate warming. A small hysteresis is observed.

of pore sizes inevitably present in the packed-powder structure. The rate of cooling or warming did not seem to be crucial if one allowed an hour or two to go through the transition region. The temperatures of the  $^3\text{He}$  and  $^4\text{He}$  refrigerators were kept equal over most of the temperature range, to attain a constant temperature over the entire sample. Below about 1.2 K, the ends of the Carbolac-filled region were left at the bottom temperature obtainable by the  $^4\text{He}$  refrigerator as the  $^3\text{He}$  refrigerator continued to cool, leaving perhaps 10% of the sample volume actually at a somewhat higher temperature. However, as very small pressure changes were taking place in this temperature range anyway, this should make a negligible correction to the low-temperature data. The data is in qualitative accord with related data taken on Vycor by the Florida<sup>18</sup> and Sussex<sup>19</sup> groups. However, in the Florida experiment the sample cell was filled to a 50% packing fraction with granular Vycor, so that the majority of the helium was in the bulk, but in contact through short diffusive paths with that in the granules.

The cell used in the Florida experiments was connected by a relatively weak thermal link to the refrigerator, so that effectively latent heat associated with freezing could also be measured, and in addition a second heat capacity anomaly which they associated with the superfluid transition. It should be noted that earlier experiments<sup>1</sup> at lower pressures have found that the peak in the heat capacity for helium in confined geometries occurs at a higher temperature than the onset of superflow. Our experiments observed a broader temperature range for the freezing transition, but a substantially smaller hysteresis than the Florida experiments between the melting and freezing behavior. Because of the unavailability of thermal measurements, the heat-capacity signature of the superfluid transition could not be observed. These measurements

were in reasonable, qualitative agreement with the flow experiments through the same medium, showing a comparable degree of supercooling before the beginning of freezing. They also gave a better idea of the breadth of the region over which solid formation was occurring, as the flow experiments essentially gave a value for complete blockage of the flow channels. A further use of the Carbolac-filled pressure transducer was to check for pressure equilibrium between the interior of the superleak and the external bulk helium in the presence of a temperature gradient. It was verified that the pressure gradient arising from the thermomechanical effect was in fact no more than 0.1 to 0.2 bar over the range of interest, small in comparison with the observed suppressions of solidification.

#### IV. TORSIONAL OSCILLATOR MEASUREMENTS

The flow measurements described in Sec. II demonstrated that superflow takes place in sufficiently narrow geometries at pressures higher than the bulk solidification pressure. However, they could only be used in a restricted part of the phase diagram, and yield limited information.

To extend the range and type of information on this new state of superfluid  $^4\text{He}$  we carried out a second series of experiments with a torsional oscillator of a type similar to that used by Berthold *et al.*<sup>8</sup> and by Bishop *et al.*<sup>9</sup> for measuring the temperature dependence of the superfluid mass of  $^4\text{He}$  in the adsorbed and bulk liquid states of  $^4\text{He}$  in Vycor. We have also been able to make some interesting observations with the same apparatus using  $^3\text{He}$ , which is not superfluid at the temperatures of our experiments. The oscillator, shown in Fig. 9, is a hollow cylinder of beryllium copper, 11 mm in diameter and 11 mm long, almost completely filled with a cylinder of Vycor porous glass which is firmly sealed into it with a thin film of Stycast 1266. This vessel, together with the

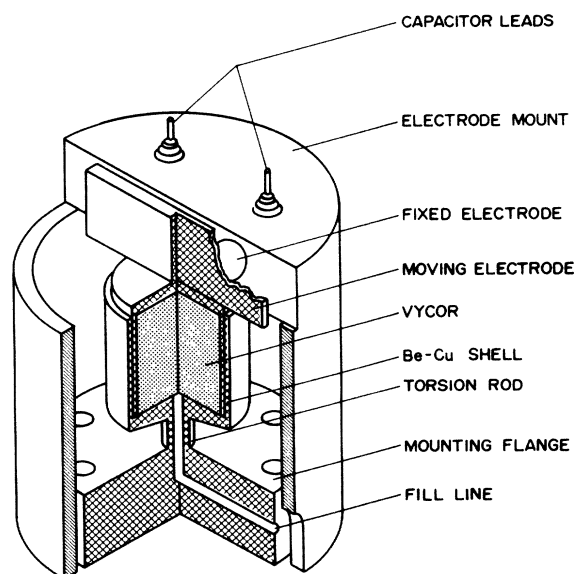


FIG. 9. Schematic view of the torsional oscillator and the detector assembly, with a partially cut-away section.

Vycor and any helium entrained with it, form the moment of inertia of the oscillator. Helium is admitted to the Vycor through the hollow beryllium copper tube, of 1 mm bore and 3 mm o.d., which also forms the torsion rod of the oscillator. The rod is connected to a massive solid copper cylinder which filters out vibrational noise. A carbon resistance thermometer on the cylinder measures its temperature and that of the torsional oscillator, and a copper thermal link to the refrigerator above ensures that, at the higher pressures, a solid block of helium forms at the inlet to the cylinder of the narrow filling capillary so that there is only a small dead volume of bulk helium associated with the measured system. The quality factor,  $Q$ , of the empty oscillator, which had been heat treated in an argon atmosphere, was  $\sim 6 \times 10^5$  at a resonance frequency of 3.3 kHz at 1 K.

The oscillator is driven and its motion is detected electrostatically. A cylindrical brass structure (Fig. 9) consists of two circular capacitor plates embedded in Stycast for electrical insulation, with a flat rectangular capacitor plate facing them on the oscillator top: these provide the drive and detection system. The flat rectangular electrode is made from Stycast thinly coated with electrically conducting silver paint. This electrode ( $E1$  in the block diagram of Fig. 10) is biased to 250 V by a Farrell Power Supply. When necessary it was shorted to ground with a  $0.1\text{-}\mu\text{F}$  capacitor to reduce microphonic noise caused by vibration of the high-voltage lead. The torsional motion of the central electrode induces a voltage which is picked up by electrode  $E2$  in Fig. 10 and amplified by an Ortec-Brookdeal differential ac amplifier. The signal is also monitored by an Ortec-Brookdeal lock-in amplifier and displayed digitally by a Fluke digital voltmeter. Since the cell is operated at constant drive, the detected amplitude is directly proportional to the  $Q$  of the torsional oscillator.

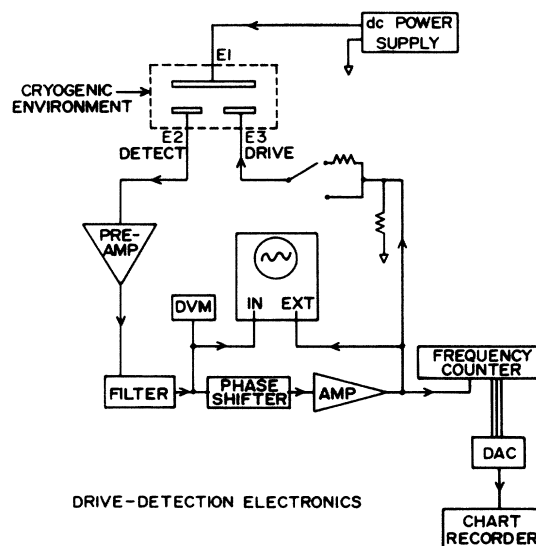


FIG. 10. Torsional oscillator drive and detection electronics.

The amplifier output is also fed in turn into a Barr-Stroud active filter, a phase shifter, and a low-noise amplifier working at saturation as a zero-crossing detector. The signal is then fed back to electrode *E3* (Fig. 10) to drive the oscillator. This type of circuit provides a drive mechanism which is independent of the amplitude of the oscillator.

The signal frequency is counted using a Hewlett-Packard Universal Counter, averaging over  $10^5$  counts in  $\sim 30$  sec. The counter output is analogue converted and displayed on a chart recorder. The frequency and thermometric data are also processed with a parallel counter using an Arcturus 18D computer.

#### A. Torsional oscillator results— $^4\text{He}$

The period  $P$  of the oscillator is given by  $P = 2\pi(I/k)^{1/2}$ , where  $k$  is the rigidity modulus of the torsion tube and  $I$  is the total moment of inertia including beryllium-copper container, Vycor, bulk helium in dead spaces in the oscillator, and helium in the Vycor pores which is entrained with the oscillator. When the helium is solid, or in the normal liquid state where the viscous penetration depth is much larger than the pore size, it contributes all of its mass to the moment of inertia. Below the superfluid transition it becomes partly decoupled, and the transition is marked by a sharp drop in period.

Figure 11 shows a series of period measurements as a function of temperature for six different pressures in the region below the bulk melting curve, where the helium everywhere in the cold region is in the liquid state and is directly connected to a precise gauge where its pressure can be measured. The oscillator was filled at 4.2 K, and at each pressure the temperature was reduced step by step to the values shown in the figure, waiting at each temperature for times of at least an hour. During this period, while waiting for equilibrium, the pressure was adjusted to maintain the initial value. Because small variations in the absolute values of the oscillator period at a particular pressure at 4.2 K were observed to occur for time on the order a day, a single run was made, lasting a few hours, of the period as a function of pressure at 4.2 K, and the values shown in Fig. 11 have been normalized to give the same pressure variation as in that run.

All of the curves in Fig. 11 show the same general characteristics. Between the highest temperatures and temperatures such as that marked *a* at the highest pressure where it is clearest, the period increases slightly. This increase, corresponding to an increasing moment of inertia, indicates that the volume of helium in the oscillator at constant pressure decreases with decreasing temperature, i.e., that the isobaric expansion coefficient of  $^4\text{He}$  in Vycor is positive in this region, as it is in the bulk phase.

At points such as *a*, a slight decrease in period is observed down to a much more sharply defined drop at points such as *b*. The points *a* are found to correspond rather well with the onset of superfluidity in bulk liquid  $^4\text{He}$  (note that these are not quite the same as those of the density maxima, which occur several millikelvin higher).

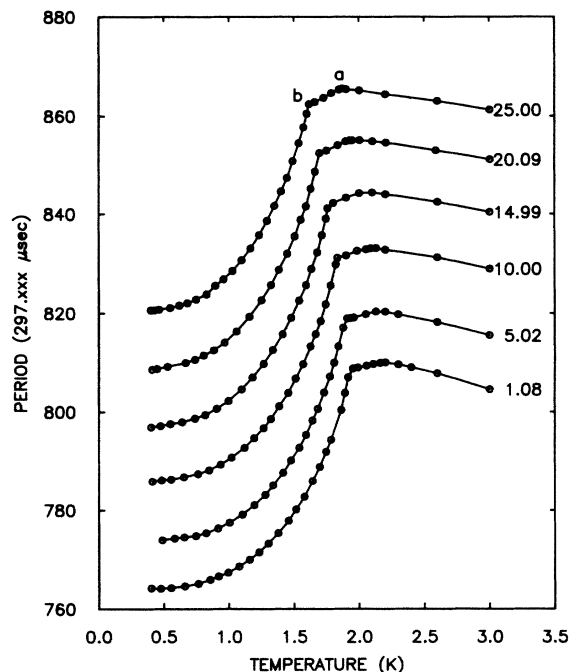


FIG. 11. Variation of oscillator period with temperature for  $^4\text{He}$  at several different pressures in the bulk fluid region. The ordinates, from 760 to 880, are the last three digits XXX in the total period 297.XXX  $\mu\text{sec}$ .

We attribute the small decrease in period between points *a* and *b* as being due to decoupling of the superfluid component of the small amount of bulk  $^4\text{He}$  which is unavoidably present in the oscillator, including that in the 1-mm bore of the torsional tube and any other accidentally present in the main body of the oscillator itself. In view of the uncertainty and small amount of this bulk liquid we do not expect to be able to compare precisely the drop in  $P$  with the expected amount, but in order of magnitude it corresponds to the relatively well-known volume in the torsion tube, indicating that the amount of bulk dead space in the rest of the oscillator is quite small.

The sharp decrease in period at points *b* is attributed to the onset of superfluidity within the pores of Vycor itself. In a similar way to the well-known variation of the normal fluid fraction in bulk He II, it can be seen that the superfluid fraction increases progressively as the temperature is decreased, and becomes very nearly constant below  $\sim 0.5$  K. Also, as with bulk liquid, the normal fluid fraction increases with pressure at a given temperature corresponding to an increase in the elementary excitations which constitute the normal fluid. Because of the restricted geometry of the Vycor, which limits the wavelength spectrum of normal phonon modes available (the predominant excitations at low temperatures), we do not expect this to parallel exactly what is found in bulk liquid. Moreover, because of the tortuous nature of the pore structure a certain fraction of the pore walls have a component perpendicular to the superfluid motion, and some of the superfluid will therefore be entrained with the oscil-

lator motion. We shall return to a further discussion of these questions later, while remarking here that we do nevertheless expect some direct relationship between the change in period of the oscillator from the Vycor transition  $b$  to its value extrapolated to zero temperature, and the change in superfluid mass over the same temperature interval. In a later figure (13) we show how  $T_0$ , the onset temperature for superfluidity in this specimen of Vycor, varies with pressure: It is closely parallel to the bulk liquid  $\lambda$  line and to a similar onset temperature line (not shown) observed for a different Vycor sample by Bishop *et al.*<sup>9</sup>

When the initial pressure of the experiments (at 4.2 K) is above that of the minimum solidification curve pressure, different behavior is observed, shown in Fig. 12 (note that, in order to avoid additional and unnecessary complication to the observations, we always started with initial pressures which were above that of the intersection of the bulk  $\lambda$  line with the melting curve). With decreasing temperature the period increases, as before, until at a sufficiently low temperature the bulk solidification curve is encountered. At this point we expect a block of solid helium to form at the entrance to the massive copper cylinder (Fig. 9) and that at lower temperatures our observations

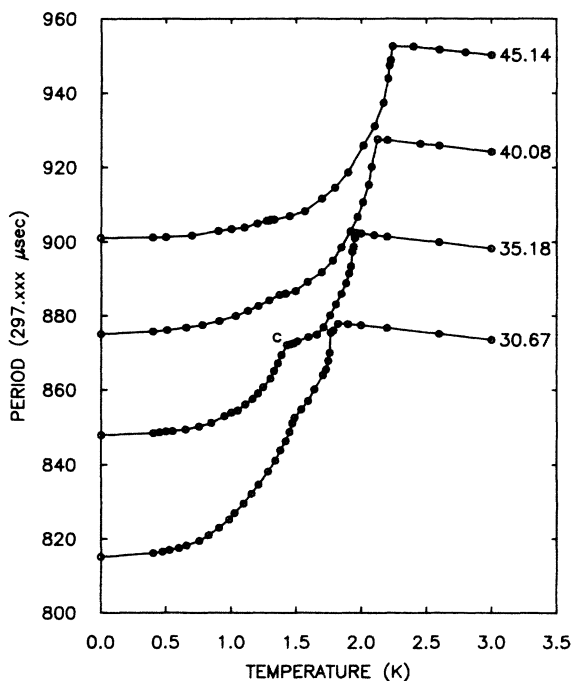


FIG. 12. Variation of oscillator period with temperature for  $^4\text{He}$  at several different pressures above  $p_m$ . The ordinates, from 800 to 920, are the last three digits XXX in the total period 297.XXX  $\mu\text{sec}$ . These curves have been displaced from one another to avoid visual confusion caused by crossings. The number to the right of each curve gives its pressure in bars, and the ordinates refer to the 30.67-bars curve. Successively higher pressure curves have been moved upward by 20, 40, and 50 nsec units.

will all relate to a constant mass of helium between this point and the rest of the oscillator system. Unexpectedly, we find that when the system reaches the melting curve the period drops sharply (Fig. 12), accompanied by an increase in dissipation. We do not fully understand this effect, which also occurs with  $^3\text{He}$ , and we return to it later. It does not affect observations of the superfluid transition and allowance can be made for it in calculating the change in period due to decoupling of the superfluid.

At lower temperatures still, another sharp drop in period is observed at points such as that marked  $c$ , which we associate with a transition to superfluidity within the Vycor, occurring at pressures within the bulk solid-phase region of the phase diagram. These transition temperatures are plotted in the phase diagram of Fig. 13, which shows that the superfluid onset temperature in Vycor is propagated up from the liquid state well above the bulk solidification pressure,<sup>9,14</sup> before the last indication of the transition disappears at the highest pressures. Since in the present experiment we have no direct observation of the pressure within the Vycor when the filling line is blocked with solid, we have plotted the data above the bulk solidification curve using the observed pressure at block-off, which is an upper limit. Data obtained in other laboratories<sup>18,20</sup> after these experiments were done, also shown in the figure, are quite consistent with these within the limits of accuracy.

We conclude from the measurements described in this

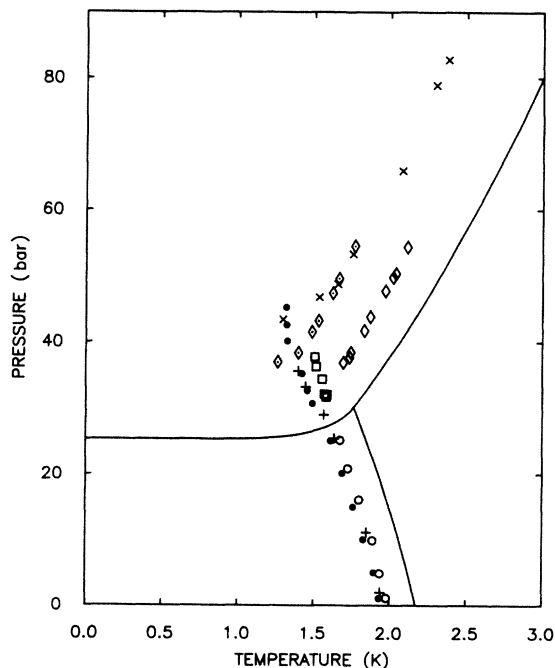


FIG. 13. Phase diagram for  $^4\text{He}$ . The bulk solidification curve and  $\lambda$  line are indicated by solid lines. Data shown are our results for the onset of superflow in Vycor ( $\circ$ ), Ref. 14, and the data of various other researchers: onset of superflow ( $\circ$ ), Bishop *et al.*, Ref. 9; freezing ( $\times$ ) and onset of superflow ( $+$ ) Beamish *et al.*, Ref. 20; freezing ( $\diamond$ ), melting ( $\diamond$ ), and onset of superflow ( $\square$ ), Adams *et al.*, Ref. 18.



paper that in narrow pores and in small spaces between powder granules, a liquid phase of  $^4\text{He}$  can exist at pressures significantly higher than bulk solid. This conclusion is now well supported by work of other authors quoted above. Also shown in Fig. 13 is the band of pressures that encompasses the "internal melting curves" for Vycor: This is a range of pressures rather than a single curve because of the pore size distribution, which allows solid to form at lower pressures in the larger pores, and has been derived from these and a number of experiments by other authors.

### B. Torsional oscillator measurements— $^3\text{He}$

As a check on some of the observations reported above with  $^4\text{He}$ , we repeated the oscillator experiments using  $^3\text{He}$ , which does not become superfluid in the temperature region of these experiments. Since in all conditions of the observations the viscous penetration depth is much greater than the pore diameter, we would not expect any large changes in period as the temperature is reduced at constant pressure, other than those resulting from the isobaric expansion coefficient. This is borne out by the results shown in Fig. 14 for pressures below  $p_m$ , i.e., in the bulk fluid region. At starting pressures higher than  $p_m$ , however, as shown in Fig. 15, we observe the same phenomenon as in  $^4\text{He}$ , that is a sharp drop in period which occurs just as the bulk solidification curve is reached. The variation with temperature is similar to that found with  $^4\text{He}$ , and the period levels off at the lower temperatures without, of course, exhibiting the additional decrease due to the superfluid transition found with  $^4\text{He}$ .

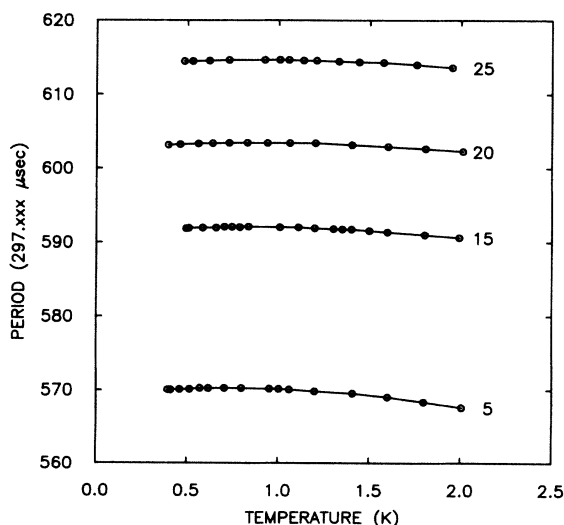


FIG. 14. Variation of oscillator period with temperature for  $^3\text{He}$  at various pressures in the bulk fluid region. The ordinates 560 and 620 are the last three digits XXX in the total period 297.XXX  $\mu\text{sec}$ .

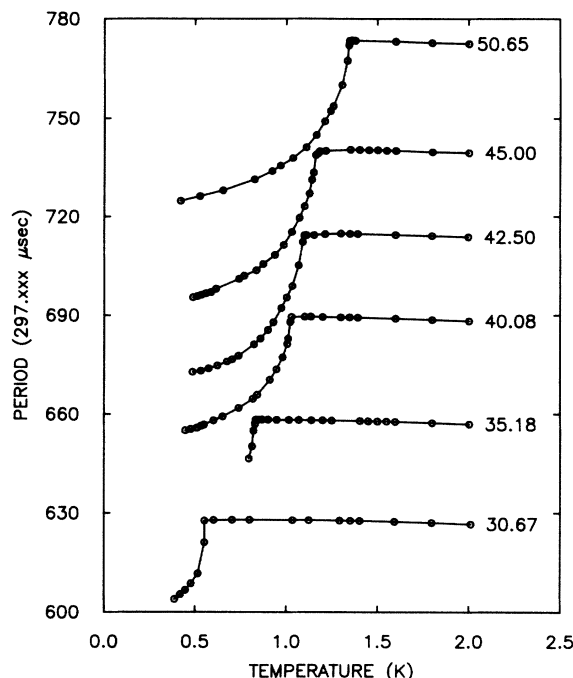


FIG. 15. Variation of oscillator period with temperature for  $^3\text{He}$  at various pressures above the melting-curve minimum pressure. The ordinates 600 to 680 are the last three digits XXX in the total period 297 XXX  $\mu\text{sec}$ . As in Fig. 12, the curves have been displaced to avoid crossings. The number to the right of each curve gives its pressure in bars, and the ordinates refer to the 30.67-bars curve. The successively higher pressure curves have been displaced upward by 20, 40, 60, 80, and 100 nsec units.

## V. DISCUSSION

### A. Existence of fluid above bulk solidification pressure

Two suggestions have been put forward for the existence of a fluid state in a region of the phase diagram where in the thermodynamic limit the solid phase would be stable. In our original work we noted that it had already been observed, in interfacial tension measurements between solid and liquid  $^4\text{He}$  and substrates of copper and glass, that the substrate-liquid free energy was higher than that of the substrate-solid, so that it was the liquid, rather than the solid, that wetted the wall surface.<sup>11</sup> With the assumption that this was also true for the He-Vycor pore interface, we reasoned that solid would not preferentially nucleate on the Vycor walls at  $p > p_m$ , but would nucleate instead within the small fluid region of the pores. The probability of a density fluctuation nucleating a solid droplet is well known<sup>28</sup> to be proportional to  $\exp(-W/k_B T)$  where  $W$  is the work needed to form a nucleus. The latter, which provides a potential barrier against the formation of a solid nucleus, contains a volume term proportional to  $r^3$  and a competing term proportional to  $r^2$ . Its minimum occurs at a critical radius

$$r_c = \frac{2\gamma_{ls}}{\Delta p} \frac{V_s}{V_l - V_s}, \quad (1)$$

where  $\gamma_{ls}$  is the interfacial tension between liquid and solid,  $V_s$  is the solid molar volume and  $V_l$  the liquid volume under the prevailing temperature and pressure conditions, and  $\Delta p$  is the excess pressure above bulk solidification pressure needed to stabilize the nucleus. Nuclei of smaller radius decay, nuclei of larger radius grow. Thus we picture the fluid above bulk solidification pressure as being in a metastable state in which density fluctuations continually attempt to form stable nuclei but are unable to do so until the excess pressure reaches the value given by Eq. (1) with  $r_c$  equal to the effective pore size (which varies). In this model the high-density nuclei form within the liquid matrix, and no explanation is provided for the failure of solid to wet the Vycor glass walls, except that the structure of crystalline helium is incommensurate with the glassy state of the Vycor pore surface. It does provide a qualitative explanation of the increased lossiness at the solidification curve, since it is at these points that finite-density fluctuations begin to occur within the pores which may oscillate out of phase with the Vycor cylinder. Such out-of-phase oscillations could, in principle, provide a mechanism for the drop in period when the melting curve is encountered in both  $^3\text{He}$  and  $^4\text{He}$ , but not enough is known about the system, and it is probably too complex geometrically for a detailed analysis to be made.

If we take bulk liquid values for  $V_s$  and  $V_l$  on the melting curve at the same temperature, our measured  $\Delta p$  gives  $\gamma_{ls} \approx 0.31 \text{ erg cm}^{-2}$ , which is about a factor 2 greater than the measured value of Landau *et al.*,<sup>29</sup> and about the same as Beamish *et al.*<sup>20</sup> Adams *et al.*,<sup>18</sup> using their measured  $\Delta V_s$  for their Vycor at 32 bars and 1.3 K (instead of the bulk  $\Delta V$ ) obtained  $\gamma_{ls} = 0.08 \text{ erg cm}^{-2}$  which is about a factor of 2 less than the observed value  $\gamma_{ls} = 0.16 \text{ erg cm}^{-2}$ .

A more detailed model has been proposed by Dash<sup>27</sup> to explain microscopically the observation that the liquid-substrate free energy is less than that of the solid-substrate for certain substrates. He suggests that the solid-substrate free energy is enhanced, on disordered surfaces, by the grain boundary energy. Detailed estimates of the enhancement lead to a value for the additional pressure needed to nucleate solid on the surface of a porous or granular material of

$$\Delta p \approx 0.05\alpha\mu a/l, \quad (2)$$

where  $a$  is the lattice spacing of the crystal,  $\mu$  is its shear modulus,  $l$  is the volume to surface ratio of the pores ( $\sim \frac{1}{2}$  of the effective "pore radius" for Vycor), and  $\alpha$  is a proportionality constant related to surface roughness, and, in powders, to the packing geometry. For Vycor, we would have  $\alpha \sim 10$  for our excess pressure of 15.3 bars at an initial 40-bars pressure.

Both models gives reasonable accounts of the results, but it should be noted that, although in both of them similar reasons are given—quantitative in the case of Dash's model—for the preference of liquid rather than solid to wet the substrate, they are radically different in

implication. In Dash's model, the solid does still nucleate at the substrate, whereas in our model it nucleates as a density fluctuation within the fluid which can become stable in the right thermodynamic conditions. In Dash's model it is difficult to see why additional loss should occur on encountering the solidification curve (apart from a short time-dependent effect while fluid moves to the wall), whereas in our fluid nucleation model it can be more naturally understood as the movement of density fluctuations within the fluid matrix in which they are formed.

#### B. Variation of superfluid mass within Vycor above solidification pressures

With a simple and well-defined oscillator geometry, measurements of the change in period can, in principle, be used to calculate changes in superfluid mass through the equation  $P = 2\pi(I/k)^{1/2}$ , without a knowledge of the torsion constant  $k$ . For a number of reasons we cannot do so in the present case with reasonable certainty. The most significant of these is the complex geometry of the Vycor itself. As already pointed out, the tortuous paths connecting the pores, and the presence of blind pores, lead to entraining of superfluid, and to a contribution to the moment of inertia, which is not known and cannot be estimated with any certainty. It is related to the tortuosity factor estimated from spin-diffusion measurements of  $^3\text{He}$  in Vycor,<sup>30</sup> which is  $\sim 0.3$  at SVP at low temperatures, but this can be both temperature and pressure dependent, for two different reasons which we now outline.

The actual path for superfluid flow around a given path in the Vycor cylinder is longer than the geometrical path calculated as  $2\pi$  times the radius of the path, and is temperature dependent because the onset temperature for superflow depends on channel size which varies around a superfluid flow path; this can be a particularly strong effect near the onset temperature for superflow where the superfluid coherence length, whose value compared with the channel diameter determines the onset temperature, diverges. At temperatures away from the onset temperature it is probably not an important effect.

The pressure dependence of the tortuosity factor is particularly significant in these experiments at pressures above the bulk solidification pressure. In this case, the larger pores in a superfluid circulation path will tend to block with solid at lower pressures than the smaller ones, changing the effective superfluid flow path. At pressures below bulk solidification pressure, a similar effect occurs, but in this region increasing pressure tends to make the smaller pores go normal first.

In addition to these effects of Vycor geometry, there are uncertainties in calculating the superfluid mass due to dead volumes in the oscillator with essentially bulk dimensions. We have already pointed out the effect of these on the superfluid transitional region at  $p < p_m$  in Fig. 11, and at  $p > p_m$  in Fig. 12. In both cases, we can make semiempirical corrections for these effects from the observations themselves, but in view of the inherent uncertainties in the Vycor geometry we do not feel justified in converting our period variations into quantitative superfluid

mass variations, although it is possible to draw some interesting conclusions.

These corrections for bulk superfluid contributions, and for the decrease in period on encountering the solidification curve whose origin is unknown, can be made as illustrated in the schematic diagrams of Figs. 16(a) and 16(b). The first of these represents the observations below the lowest solidification pressure, i.e., where the bulk phase is entirely liquid. The part *ab* of the curve is attributed, as already explained, to decoupling of bulk liquid in the oscillator, mainly in the bore of the torsion tube. This part is extrapolated to absolute zero, as is the part below point *b*, which represents the decrease in moment of inertia of the coupled part of the helium in Vycor plus that in bulk. The difference between these, labeled  $\Delta P_v(0)$  in the figure, is the change of period due to decoupling of superfluid  $^4\text{He}$  in this specimen of Vycor at 0 K and at the pressure of the observations.

A similar procedure, illustrated in Fig. 16(b), is followed for the case where the bulk freezing pressure is encountered first, at point *m* in the figure. The curve *mc* is fitted to a suitable algebraic expression and extrapolated to absolute zero. In this case, all dead spaces within the oscillator are occupied with bulk solid which is locked to the oscillator, so there is no decoupling due to bulk superfluid, and the decrease in period below *c* is attributable to

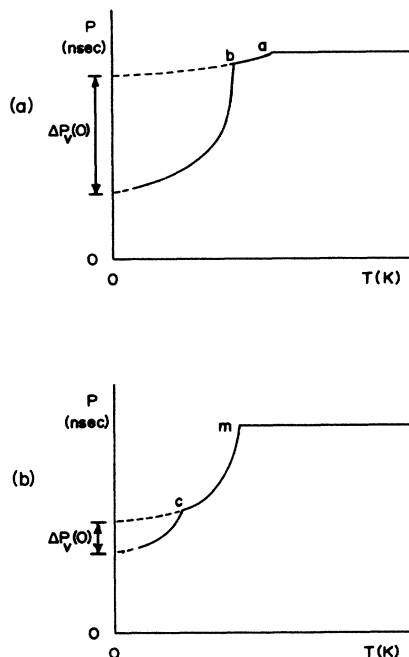


FIG. 16. (a) and (b) Schematic diagrams representing data for  $^4\text{He}$  in Figs. 11 and 12, illustrating the corrections made for (a) decoupling of bulk fluid in the oscillator at  $p < p_m$ , and (b) the decoupling, of unknown origin, on encountering the melting curve for initial  $p > p_m$ . In each case the quantity calculated,  $\Delta P_v(0)$ , is the loss in period at 0 K due to decoupling of the superfluid within the Vycor.

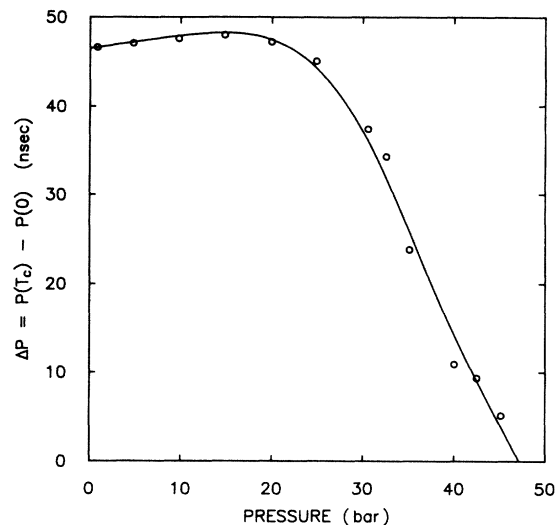


FIG. 17. The period shifts caused by decoupling of superfluid within the Vycor as a function of pressure. They have been extracted by extrapolation to  $T=0$  as explained in conjunction with Fig. 16.

the decoupling of superfluid within the Vycor, apart from the period drop due to the extrapolated part of *mc*. The part below *c* is extrapolated to 0 K, and the period decrease due to decoupling of superfluid  $^4\text{He}$  within the Vycor is again given as shown in the figure, for the pressure of the observations.

The result of these calculations is shown in Fig. 17 as the change in the period of the oscillator  $\Delta P_v(0)$  due to helium decoupling in the Vycor at absolute zero, as a function of pressure. Within the bulk fluid region of the phase diagram, i.e., up to  $\sim 25.3$  bars, the period change decreases by about 15%. Even up to about 30 bars, well into the bulk solid region of the phase diagram, the change in period does not decrease very rapidly. Thereafter, the decrease does accelerate with pressure and the superfluid signal disappears at an extrapolated pressure of about 50 bars.

In bulk liquid, all of the liquid is superfluid at absolute zero, independent of pressure, until the solidification pressure is reached. The moment of inertia of normal liquid helium would, however, increase with pressure, following the compressibility, and consequently in the bulk case the curve corresponding to Fig. 17 would increase with pressure up to the solidification pressure. In the restricted Vycor geometry the result is therefore noticeably different. Our interpretation of these results is that the superfluid signal decreases due to a decreasing superfluid mass which can have the additional effect of decreasing the connectivity of the superfluid bath. We noted in the Introduction to this paper (Sec. I) that in a compressional cooling experiment<sup>5</sup> with  $^3\text{He}$  in Vycor, a high-density state (greater than solid density) with high entropy (i.e., disordered) had been observed close to the solidification pressure, and the possibility was later discussed<sup>31</sup> that this might be a low-dimensional state with a large number of

defects, similar to the state discussed by Guyer.<sup>32</sup> It is possible that the present observations may have a similar interpretation, with superfluid becoming replaced, as the pressure is increased, by high-density helium in an amorphous state even at the absolute zero.

#### ACKNOWLEDGMENTS

We are grateful to Dr. W. S. Truscott and Dr. T. M. Sanders for several discussions, and to Dr. C. L. Reynolds for suggesting a connection with size-dependent melting of metals. The work was carried out with partial support from United Kingdom Science and Engineering Research

Council (SERC) Grants No. GR/A7526.2 and No. GR/B/65137, from the National Science Foundation through Grants No. DMR-77-24221 and No. DMR-78-026555, by the National Science Foundation through the Cornell University Materials Science Center through Grant No. DMR-76-81083-A02, Technical Report No. 4497, and by North Atlantic Treaty Organization (NATO) Research Grant No. 0201/82. One of us (J.D.R.) acknowledges support from SERC and would also like to thank the John Simon Guggenheim Memorial Foundation for support. C.L.Z. was supported by the Royal Society/Chinese Academy of Sciences Exchange Program. D.F.B. was supported in part of this work by SERC (Grant No. B/SF/122).

\*Present address: Physics Dept., University of Science and Technology of China, Hefei, Anhui, The People's Republic of China.

†Present address: Physics Department, Hacettepe University, Ankara, Turkey.

<sup>1</sup>For reviews of multilayer adsorbed helium which are particularly relevant to this paper, see D. F. Brewer, *J. Low Temp. Phys.* **3**, 205 (1970); in *The Physics of Liquid Helium and Solid Helium, Part II*, edited by K. H. Bennemann and J. B. Ketterson (Wiley, New York, 1978), Chap. 6, and references therein.

<sup>2</sup>S. Franchetti, *Nuovo Cimento* **4**, 1504 (1956).

<sup>3</sup>J. Landau and W. F. Saam, *Phys. Rev. Lett.* **38**, 23 (1977).

<sup>4</sup>D. F. Brewer and D. C. Champeney, *Proc. Phys. Soc. London* **79**, 855 (1962).

<sup>5</sup>H. M. Mitchell, D. F. Brewer, S. Swithenby, and W. S. Truscott, *J. Low Temp. Phys.* **38**, 475 (1980).

<sup>6</sup>Various substrates have been used in these experiments. Manufacturers of these substrates are as follows: Vycor Glass, Corning Glass Works, Houghton Park, Corning, NY 14830; Carbon Black (Carbolac 1) Cabot Corporation, 125 High Street, Boston, MA 02110; 200 Å Rouge (Sicotrans Red 400) BASF Wyandotte Corporation, P.O. Box 181, Parsippany, NJ 07054; 500 Å, 3000 Å Alumina, Linde Crystal Products Dept., 8888 Balboa Avenue, San Diego, CA 92123; 500 Å Nuclepore Filter, Nuclepore Corporation, 7035 Commerce Circle, Pleasanton, CA 94566; DLX6000 Fluorocarbon, E. I. duPont de Nemours and Co., Inc., Plastic Products and Resins Department, Wilmington, DE 19808.

<sup>7</sup>D. F. Brewer, A. J. Dahm, J. Hutchins, W. S. Truscott, and D. N. Williams, *J. Phys. (Paris) Colloq.* **39**, C6-351 (1978).

<sup>8</sup>J. E. Berthold, D. J. Bishop, and J. D. Reppy, *Phys. Rev. Lett.* **39**, 348 (1977).

<sup>9</sup>D. J. Bishop, J. E. Berthold, J. M. Parpia, and J. D. Reppy, *Phys. Rev. B* **24**, 5047 (1981).

<sup>10</sup>D. D. Osheroff, Ph.D. thesis, Cornell University, 1972 (unpublished).

<sup>11</sup>S. Balibar, D. O. Edwards, and C. Laroche, *Phys. Rev. Lett.* **42**, 782 (1979).

<sup>12</sup>F. Scaramuzzi, A. Savoia, D. L. Goodstein, and M. W. Cole,

*Phys. Rev. B* **16**, 3108 (1977).

<sup>13</sup>E. N. Smith, D. F. Brewer, Cao Liezhao, and J. D. Reppy, *Physica* **107B**, 585 (1981); *Bull. Am. Phys. Soc.* **26**, 632 (1981).

<sup>14</sup>D. F. Brewer, Cao Liezhao, C. Girit, and J. D. Reppy, *Physica* **107B**, 583 (1981).

<sup>15</sup>A. L. Thomson, D. F. Brewer, T. Naji, S. Haynes, and J. D. Reppy, *Physica* **107B**, 581 (1981).

<sup>16</sup>A. L. Thomson, D. F. Brewer, and S. Haynes (unpublished).

<sup>17</sup>E. N. Smith and J. D. Reppy, *Bull. Am. Phys. Soc.* **27**, 556 (1982).

<sup>18</sup>E. D. Adams, K. Uhlig, Yi-Hua Tang, and G. E. Haas, *Phys. Rev. Lett.* **52**, 2249 (1984); and private communication.

<sup>19</sup>A. L. Thomson, D. F. Brewer, and S. Haynes, *Proceedings of the 17th International Low Temperature Conference LT17* (North-Holland, Amsterdam, 1984), p. 525.

<sup>20</sup>J. Beamish, A. Hikata, L. Tell, and C. Elbaum, *Phys. Rev. Lett.* **50**, 425 (1983).

<sup>21</sup>M. Shimoda, T. Mizusaki, T. Suzuki, A. Hirai, and E. Eguchi, *Phys. Lett.* **102A**, 426 (1984); and private communication.

<sup>22</sup>M. J. Lea and P. Fozzomi, *J. Low Temp. Phys.* **56**, 25 (1984).

<sup>23</sup>E. R. Grilly, *J. Low Temp. Phys.* **11**, 33 (1973).

<sup>24</sup>H. A. Kierstead, *Phys. Rev.* **162**, 153 (1967).

<sup>25</sup>T.-p. Chen, M. J. DiPirro, B. Bhattacharyya, and F. M. Gasparini, *Rev. Sci. Instrum.* **51**, 846 (1980).

<sup>26</sup>See, for example, V. Gridin, J. Adler, Y. Eckstein, and E. Polturak, *Phys. Rev. Lett.* **53**, 802 (1984), and references therein.

<sup>27</sup>J. G. Dash, *Phys. Rev. B* **25**, 508 (1982).

<sup>28</sup>Landau and Lifshitz, *Statistical Physics*, 3rd ed., edited by E. M. Lifshitz and L. P. Pitaevskii (Pergamon, Oxford, 1980), Chap. XV, Sec. 162.

<sup>29</sup>J. Landau, S. G. Lipson, L. M. Määttänen, L. S. Balfour, and D. O. Edwards, *Phys. Rev. Lett.* **45**, 31 (1980).

<sup>30</sup>D. F. Brewer and J. S. Rolt, *Phys. Lett.* **48A**, 141 (1974).

<sup>31</sup>W. S. Truscott and D. F. Brewer, *J. Phys. (Paris) Colloq.* **41**, C7-267 (1980).

<sup>32</sup>R. Guyer, in *Proceedings of the Conference on Ultralow Temperatures, Hakoné*, edited by T. Sugawara, S. Nakajima, T. Ohtsuka, and T. Usui (Japanese Physical Society, Tokyo, 1977), p. 178.

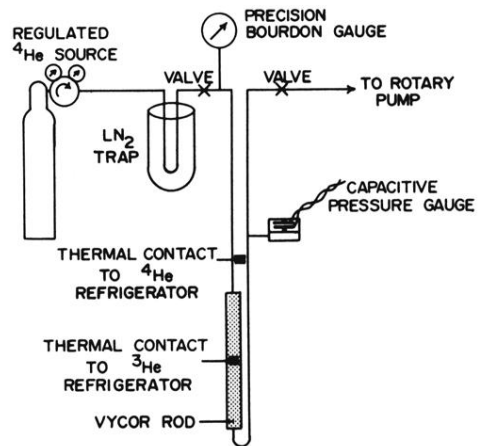


FIG. 1. Schematic diagram of flow apparatus used in initial experiments.

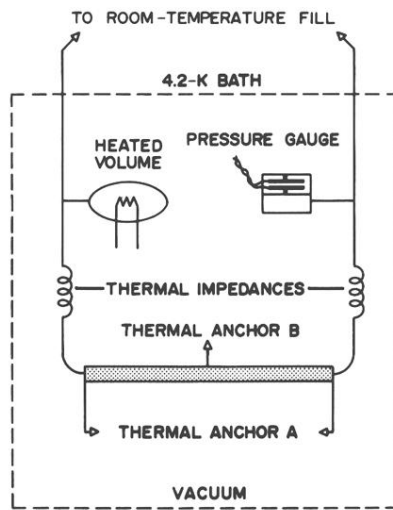


FIG. 3. Modified apparatus, with separate volume and heater used to create small pressure fluctuations at low temperatures.

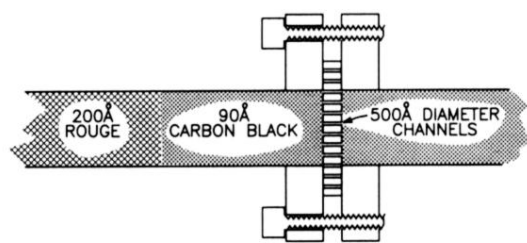


FIG. 6. Schematic view of apparatus for examining solid suppression in a piece of Nuclepore filter sandwiched between packed powder, not to scale. The thin sheet of filter paper serves both as a set of flow channels, and as a gasket sealing between the superleak and the vacuum can.

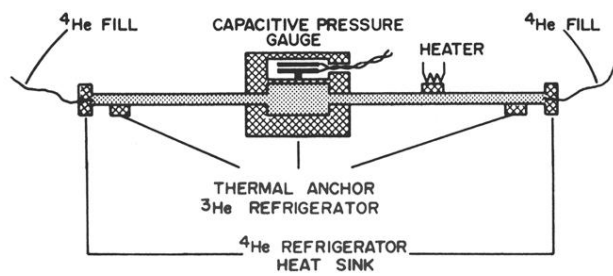


FIG. 7. Apparatus used for measurement of  $p(T)$  at constant volume for  ${}^4\text{He}$  confined in  $90\text{-}\text{\AA}$  carbon black powder packed to approximately 25% packing fraction.



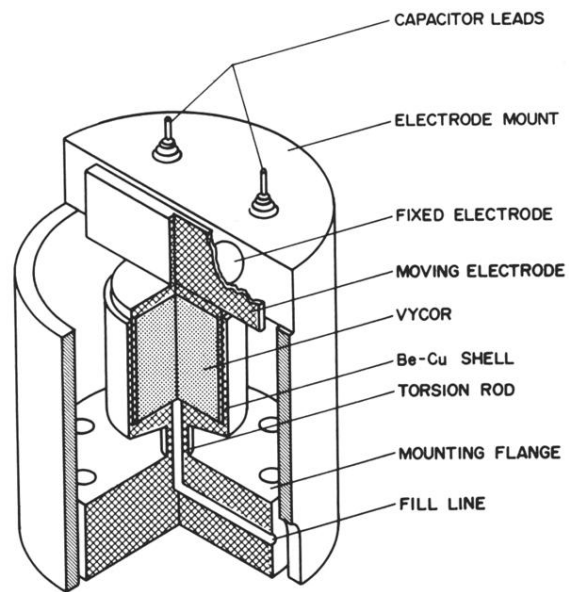


FIG. 9. Schematic view of the torsional oscillator and the detector assembly, with a partially cut-away section.